Inversion of polarization by light-induced stabilization

H. G. Weber, F. Bylicki, and G. Miksch
Physikalisches Institut der Universität Heidelberg, D-6900 Heidelberg 1, Federal Republic of Germany
(Received 27 February 1984)

We report on a new effect which is observed when the small polyatomic molecule NO_2 is prepared under collision-free conditions into an electronically excited state. As the intensity of the exciting laser light is varied, the degree of polarization of the fluorescence light may undergo a change in sign. The analysis of the experimental results confronts us with an interesting problem concerning the time evolution of an isolated polyatomic system. In this paper we present the experimental results and a simple model which successfully describes these results. According to this model, the inversion of the polarization of the fluorescence light is a consequence of light-induced stability of the optically prepared state.

I. INTRODUCTION

In this paper we report on a new effect which is observed when the small polyatomic molecule NO_2 is prepared into an electronically excited state by light absorption. Preparing an atom into an excited state by light absorption seems to be a well-understood problem (see, for instance, Refs. 1 and 2). This is obviously not so in a small polyatomic system like NO_2 as we will show in this paper. NO_2 is supposed to have a sparse level structure (compare Refs. 3 and 4 and references given therein). Using a narrow-band laser and molecular beam conditions we expect therefore a situation similar to atoms, namely, preparation of the molecule into a single isolated quantum state and the subsequent radiative decay of this prepared state. However, in the present paper we report experimental results which obviously contradict this belief. The results are confronting us with a property of the optically excited state which has no analogy in atomic physics.

We report on zero-magnetic-field level crossing (Hanle effect) and optical radio-frequency double-resonance experiments. For a review of these experimental techniques compare Ref. 5. In these experiments we measure the polarization of the fluorescence light versus an external magnetic field. There appears a dramatic change in the polarization with increasing intensity of the exciting laser light. The degree of polarization changes the sign. We name this phenomenon "inversion effect." This effect on a collision-free molecule is new.

The analysis of the experimental results shows that this effect is confronting us with a fundamental problem concerning the time evolution of the free NO_2 molecule in an optically excited state.[6] A good description of the experimental results is only possible if an irreversible dynamical evolution in the excited state is assumed. In the present paper we present the experimental results of the inversion effect. We describe these results using a simple model whose rationalization will be given in a subsequent paper.[6] Some preliminary results of our investigations were reported before.[7–9]

II. EXPERIMENTAL

A schematic diagram of the experimental apparatus is shown in Fig. 1. In order to facilitate the description we introduce a coordinate system $\{x,y,z\}$. Light from a single-mode cw dye laser propagates along the y axis. The laser light, which is linearly polarized excites NO_2 molecules near the center of the coordinate system. These molecules are in a beam which propagates along the x axis. The laser-induced molecular fluorescence is seen via two photomultipliers which detect the fluorescence light emitted in opposite direction along the z axis. The polarization of the light beam and the polarization of the polarizers can be chosen appropriately. To specify these polarizations we introduce the polarization vectors e_x, e_y, and e_z which describe linear polarizations along the x, y, and z axes, respectively. Additionally, a static magnetic field B and a rf field with amplitude B_1 can be applied. The B field can be directed either along the z or the x axis. The B_1 field is linear polarized along the y axis.

The following experiments are performed.

(i) Zero-field level crossing (Hanle effect). The B field is parallel to the z axis and is swept through $B=0$. No B_1 field is present. The laser light has polarization e_x and the two polarizers have polarizations e_y and e_x,

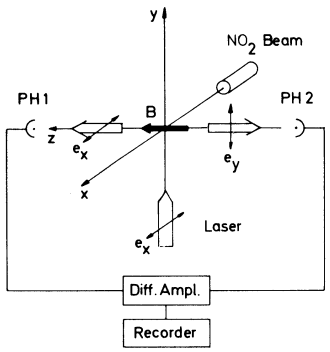

FIG. 1. Geometrical arrangement of the experimental apparatus (arrangement *i*).

respectively. This gives a Hanle signal with "absorption line shape." Using the same experimental configuration, however with the polarizations $(e_x+e_y)/\sqrt{2}$ and $(e_x-e_y)/\sqrt{2}$ of the two polarizers we obtain a Hanle signal with "dispersion line shape."

(ii) Optical-radio-frequency double resonance with π excitation. The field B is parallel to the x and is swept through a chosen field value B_0 which satisfies the resonance condition $2\pi\hbar\nu_0=g\mu_B B_0$, where ν_0 is the constant frequency of the B_1 field and $\hbar$, μ_B, and g are the Planck constant, the Bohr magneton, and the g factor of the excited state of NO_2, respectively. The laser beam has the polarization e_x and the two polarizers have the polarization e_x and e_y, respectively.

(iii) Optical-radio-frequency double resonance with σ excitation. The B field is parallel to the x axis and is swept through a chosen field value as in (ii). The laser beam has polarization e_z and the two polarizers have the polarizations e_x and e_y, respectively.

The measured signal in all experiments (except Hanle signal with dispersion line shape) is the quantity

$$S=(I_x-I_y)/(I_x+I_y) \tag{1}$$

versus the magnetic field B which is swept continuously through the desired field value in each experiment. Here I_x and I_y are the intensities of the fluorescence light with polarization e_x and e_y, respectively, detected by the two photomultipliers. We realize the measurement of S as follows. (We describe it here for a Hanle experiment. The situation is similar in the double-resonance experiment.) The laser is tuned and stabilized to a molecular transition. At a given intensity of the laser light the fluorescence intensities are $I_x'=I_y'$ with the magnetic field being out of resonance and $I_x=I_x'+\Delta I_x$ and $I_y=I_y'+\Delta I_y$ with the magnetic field being in resonance. The voltages across both photomultipliers are always (for all intensities of the laser light) adjusted to give the same constant output current I_0 of both photomultipliers with the magnetic field being out of resonance. These output currents are electronically compensated and fed (at zero voltage level) both into a difference amplifier. The output signal of the difference amplifier is therefore proportional to $I_0(\Delta I_x/I_x'-\Delta I_y/I_y')=I_0(I_x-I_y)/I_y'$ with I_0 being independent of the laser light. In general $|\Delta I_x|$ and $|\Delta I_y|$ are about 1% or less of the fluorescence intensities I_x and I_y. Therefore, Eq. (1) is well realized by this measurement procedure. It must be noted that this procedure is justified because the stray light is in general negligible and the dark current of the photomultipliers can be taken into account or totally suppressed by cooling the photomultipliers. We use rotatable polarizers. Therefore, both photomultipliers act alternatively as detectors for I_x or I_y fluorescence light. This eliminates differences in the fluorescence detection and signal procession of both detectors. Because I_x and I_y differ in general by less than 1% we will later assume

$$I_x+I_y=\tfrac{2}{3}(I_x+2I_y)=\tfrac{2}{3}I_{\text{tot}} \tag{2}$$

in the denomination of Eq. (1). I_{tot} designates the total fluorescence intensity.

In the following we describe the different components of the experimental apparatus in more detail. The vacuum chamber is constructed from stainless steel. The chamber is equipped with two liquid-nitrogen-cooled traps and two oil diffusion pumps. The background pressure in the chamber is less than 10^{-5} Torr. The beam is an effusive beam. There is no collimation. The molecules are excited ≈ 10 mm downstream from the nozzle. The nozzle is heated with a flow of warm water ($\approx 60°$C) to prevent clogging of the nozzle orifice.

The cw dye laser is a Spectra Physics Model 380 ring dye laser pumped by a Spectra-Physics Model 171 Ar-ion laser. The spectral width of the laser light is ≤ 10 MHz seen by a spectrum analyzer. The laser beam is not focused on the molecular beam. On the contrary we try to have a light beam as parallel as possible when it interacts with the molecules. The diameter of the laser beam is 1.5 mm in all experiments (if not otherwise stated).

Both photomultipliers view the NO_2 fluorescence through filters which suppress light at the laser wavelength by a factor of 10^4 and transmit the molecular fluorescence to the red. The photomultipliers are magnetically shielded. The lifetime of the optically excited molecules is about 30–50 μs. This means that equal sensitivity in the fluorescence detection over a path length of at least 5 cm is needed. In some cases where high resolution in the optical excitation is necessary the fluorescence light is seen via two slits parallel to the molecular beam.

Much care is taken in the magnetic fields, for instance into the compensation of the earth's magnetic field. But this was already described before.[10]

III. MEASUREMENTS AND RESULTS

A. Excitation spectrum

Figure 2 shows two laser fluorescence excitation spectra of NO_2 obtained under the experimental conditions described before. The total fluorescence is recorded versus the wavelength (near 593.3 nm) of the laser light. In these spectra the same upper states (the transitions 1 and 1R, etc., compare Table I) are excited either by a P-branch transition ($N+1\rightarrow N$) or by an R-branch transition ($N-1\rightarrow N$). Here N designates the quantum number of the rotational angular momentum of the excited state. The numbers in brackets written on top of some lines in the excitation spectra mark the transition in cm^{-1} (see Table I). The resolution in these spectra is ≈ 50 MHz due to the residual Doppler width in the beam. The resolution is better in the R-branch excitation spectrum than in the P-branch excitation spectrum because we improved the resolution in the R-branch excitation spectrum viewing the fluorescence through a slit parallel to the molecular beam axis. Therefore, in the R-branch spectrum the hyperfine structure underlying each line is weakly resolved (compare line 1R, for instance). With few exceptions each line in the excitation spectra corresponds to the excitation of a single fine-structure component of a single rotational state. This is clearly demonstrated in the double-resonance spectra discussed below. It should be

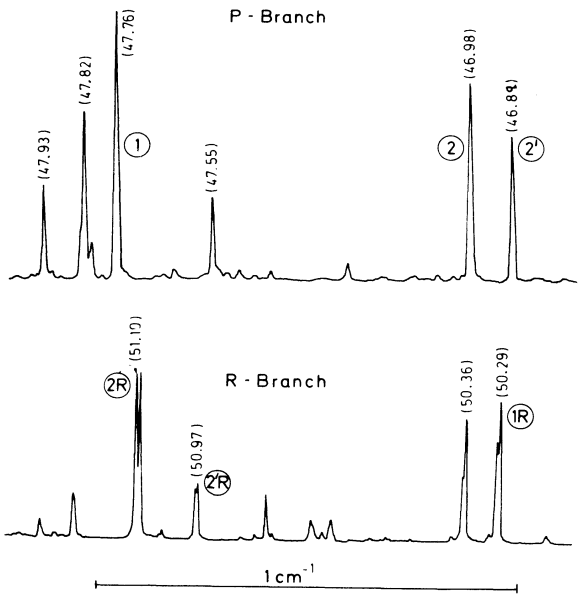

FIG. 2. Excitation spectra (R-branch and P-branch transitions near 593.3 nm). The lines numbered 1, 1R, etc., indicated transitions described in Table I.

noted that the fluorescence intensity is zero between the absorption lines. There is no continuous underground in these excitation spectra.

The rotational assignments of many transitions in the 593.3-nm band of NO_2 have been made before.[11,12] A vibrational assignment does not exist. The spectroscopy in the 593.3-nm band shows that the molecule is to a good approximation a prolate symmetric top. Each rotational state is labeled by the quantum numbers N and K_a, where K_a designates the projection of the rotational angular momentum on the figure axis of the near symmetric top. There is no degeneracy in K_a in the predominant isotopic form $^{14}N^{16}O^{16}O$ due to nuclear spin statistics. The interaction of the unpaired electron with the rotational angular momentum splits each rotational level into a fine structure doublet with $J=N\pm\frac{1}{2}$. Each of these two fine-structure levels is further split into a triplet with $F=J$ and $J\pm1$ by nuclear hyperfine interaction. The smallest spacing of levels in this structure is about 50 MHz. This level structure suggests the following coupling scheme of the angular momenta: $\hat{N}+\hat{S}=\hat{J}$ and $\hat{J}+\hat{I}=\hat{F}$, where $\hat{N}$, $\hat{S}$, $\hat{I}$, and $\hat{F}$ are the rotational, electron spin, nuclear spin, and total angular momentum operators, respectively. The optical transitions ($A\,^2B_2\leftarrow X\,^2A_1$) seem to follow the symmetric top selection rules $\Delta K_a=0$, $\Delta N=0,\pm1$ if $K_a=0$ and $\Delta N=\pm1$ if $K_a\neq0$ and $\Delta F=\Delta J=\Delta N$ on all transitions investigated here except on line 2′R. Recently we developed a method which allows us to measure simultaneously the g factors of the ground and excited state in a laser-induced transition in this molecule (13). This enables us to determine the angular momentum quantum numbers of the ground and excited state if the g factor is well behaved. These investigations give $\Delta F=\Delta J=\Delta N$ on all transitions considered here except on line 2′R.

As stated before, in most cases each line in the excitation spectrum corresponds to the excitation of a single fine-structure level. However, there are exceptions and sometimes we find overlapping lines. This is clearly seen in the double-resonance spectra because these spectra show a resolution of about 20 kHz (natural linewidth limited resolution) for states with different g factors. The double resonance experiments yield also the total angular momentum F of the excited state and F' of the ground state which are both needed for the interpretation of the experimental results (13). To simplify the description in the following we use the nomenclature: P-branch excitation ($F'=F+1\rightarrow F$), R-branch excitation ($F'=F-1\rightarrow F$) and Q-branch excitation ($F'=F\rightarrow F$) with regard to the total angular momentum. This is in agreement with the ΔN selection rule on all investigated lines except on line 2′R. Line 2′R is therefore a Q-branch transition with regard to ΔF. Most transitions investigated in this work are listed in Table I. The lines, listed in this table but not shown in the excitation spectrum in Fig. 2, may be found in the excitation spectrum depicted in Ref. 10. Table I gives also the line positions in cm^{-1}. These line positions

TABLE I. Laser-induced transition investigated in this work.

Absorption line Number	Wavelengths (cm^{-1})	Quantum numbers: Ground state N	K_a	J	F	Excited state N	K_a	J	F
1	16847.76	2	0	$\frac{5}{2}$	$\frac{7}{2}$	1	0	$\frac{3}{2}$	$\frac{5}{2}$
1R	16850.29	0	0	$\frac{1}{2}$	$\frac{3}{2}$	1	0	$\frac{3}{2}$	$\frac{5}{2}$
2′	16846.89	3	1	$\frac{5}{2}$	$\frac{7}{2}$	2	1	$\frac{3}{2}$	$\frac{5}{2}$
2′R	16850.97	1	1	$\frac{3}{2}$	$\frac{5}{2}$	2	1	$\frac{3}{2}$	$\frac{5}{2}$
2	16846.98	3	1	$\frac{7}{2}$	$\frac{5}{2}$ $\frac{7}{2}$ $\frac{9}{2}$	2	1	$\frac{5}{2}$	$\frac{3}{2}$ $\frac{5}{2}$ $\frac{7}{2}$
2	16846.98	3	2	$\frac{7}{2}$	$\frac{5}{2}$ $\frac{7}{2}$ $\frac{9}{2}$	2	2	$\frac{5}{2}$	$\frac{3}{2}$ $\frac{5}{2}$ $\frac{7}{2}$
2R	16851.10	1	1	$\frac{3}{2}$	$\frac{1}{2}$ $\frac{3}{2}$ $\frac{5}{2}$	2	1	$\frac{5}{2}$	$\frac{3}{2}$ $\frac{5}{2}$ $\frac{7}{2}$
3	16846.20	4	0	$\frac{7}{2}$	$\frac{5}{2}$ $\frac{7}{2}$ $\frac{9}{2}$	3	0	$\frac{5}{2}$	$\frac{3}{2}$ $\frac{5}{2}$ $\frac{7}{2}$
4	16846.05	4	0	$\frac{9}{2}$	$\frac{7}{2}$ $\frac{9}{2}$ $\frac{11}{2}$	3	0	$\frac{7}{2}$	$\frac{5}{2}$ $\frac{7}{2}$ $\frac{9}{2}$
7	16845.20	5	1	$\frac{11}{2}$	$\frac{9}{2}$ $\frac{11}{2}$ $\frac{13}{2}$	4	1	$\frac{9}{2}$	$\frac{7}{2}$ $\frac{9}{2}$ $\frac{11}{2}$
8	16845.10	5	1	$\frac{9}{2}$	$\frac{7}{2}$ $\frac{9}{2}$ $\frac{11}{2}$	4	1	$\frac{7}{2}$	$\frac{5}{2}$ $\frac{7}{2}$ $\frac{9}{2}$

are determined from simultaneous excitation spectra of NO_2 and I_2, using the I_2 spectral atlas of Gerstenkorn and Luc.[14] Also listed in this table are the upper state and lower state angular momentum quantum numbers. We do not present experiments using $\Delta N=0$ transitions. Experiments in this branch are difficult because it is difficult to separately excite fine-structure levels using this branch.

B. Inversion effect

Figures 3 and 4 depict Hanle signals and Fig. 5 double-resonance signals (using π excitation) on line 1. As we see, the Hanle signal changes with increasing light intensity from an upward-directed signal to a downward-directed signal with zero signal amplitude in between. This is the inversion effect. In Fig. 3, it is shown for the "absorption line shape" and in Fig. 4 for the "dispersion line shape." The double-resonance signal shows the same effect. However, contrary to the Hanle measurement in the double-resonance experiment the signal changes from downward to upward with increasing light intensity. This difference is simply a consequence of the different resonance conditions in both experiments. For high light intensity two resonances appear in the double-resonance spectrum. The strong resonance has a g factor which is in agreement (precision $\leq 1\%$) with the expected value (Hund's case b coupling) of the upper state $\langle N=1, K_a=0, J=1+\frac{1}{2}, F=J+1 |$. The much smaller resonance has a g factor belonging to the hyperfine component $F=J$. Owing to the residual Doppler width in the beam we excite both hyperfine components. There is no other resonance in the double-resonance spectrum (magnetic field scan from 0 to 100 G at the frequency $\nu=1.4$ MHz of the rf field). The hyperfine component with $F=J-1=\frac{1}{2}$ does not appear in the double-resonance spectrum (and in the Hanle signal) because a state with $F=\frac{1}{2}$ shows no fluorescence depolarization signal if excited with plane polarized light.

In the Hanle experiment it is not possible to resolve the hyperfine components. Therefore, double-resonance experiments seem to be preferable. However, the width of the double-resonance signal is mostly power broadened by the rf field and multiple rf photon transitions may influence the signal amplitude at high rf field power. Therefore, low rf-field power (and a bad signal to noise ratio) are necessary for these experiments. We could show that for low powers of the rf field the width [half-width at half maximum (HWHM)] of the double-resonance signal approaches the value $\Delta B=2$ mG corresponding to a lifetime $\tau_c=35$ μs.[10] The width (HWHM) of the Hanle signal is 4 mG independent of the light intensity in good agreement with the result of the double-resonance experiment.

If the same upper state is excited via an R-branch transition (line $1R$ in Table I) we see no inversion effect. The results of double-resonance measurements on line 1 and $1R$ are both shown in Fig. 6. This figure depicts the dependence of the signal amplitude on the light intensity for P- and R-branch excitation of the same upper state $|N=1, K_a=0, J=\frac{3}{2}, F=\frac{5}{2}\rangle$. Similar results are obtained in the Hanle experiment. The solid lines are theoretical curves which will be explained later.

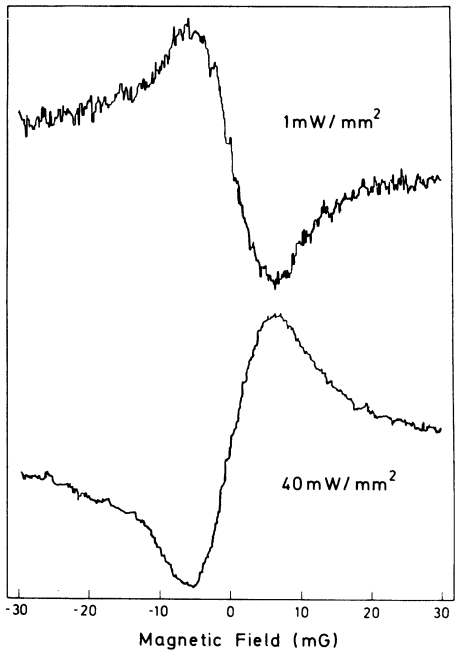

FIG. 4. Hanle signal (dispersion line shape) for two light intensities.

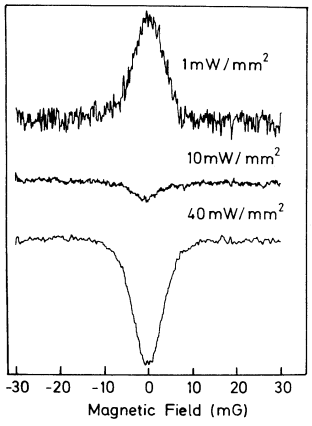

FIG. 3. Hanle signal (absorption line shape) for three light intensities.

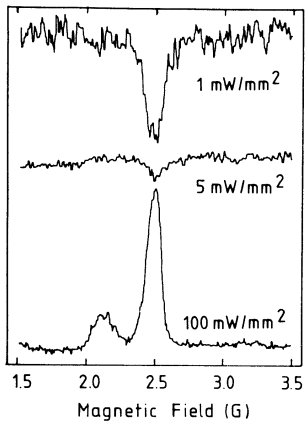

FIG. 5. Optical-rf double-resonance signal for three light intensities.

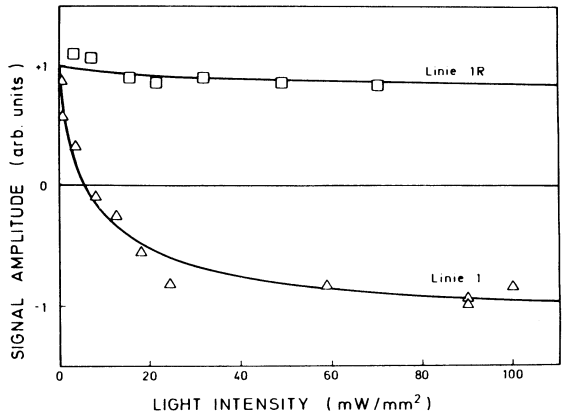

FIG. 6. Signal amplitude vs light intensity for a P-branch (line 1) and R-branch (line $1R$) transition to the same excited state with the total angular momentum $F=\frac{5}{2}$. The solid lines are theoretical curves with $A=0.1$ and $D=3$ for line 1 and $D=4$ for line $1R$. The diameter of the laser beam is about 1.5 mm in the interaction region.

The double resonance spectrum on lines $2'$ and $2'R$ shows one prominent hyperfine component. There is an inversion effect for P-branch excitation (line $2'$), but no inversion effect for the $\Delta F=0$ transition (line $2'R$). However the signal approaches $S=0$ on this line for the maximum available light intensity.

The results on line 2 correspond to those of the lines 1 and $2'$. However, the double-resonance spectrum is more complicated. On this absorption line we excite three fine-structure levels each having three hyperfine components. Thus there appear nine resonances in the double-resonance spectrum. Two fine-structure levels can well be assigned (see the quantum numbers in Table I). The third excited fine-structure level is obviously an unassigned Q-branch transition. We investigate the inversion effect on the six resonances belonging to the assigned states indicated in Table I. There is an inversion effect on the hyperfine components with $F=J$ and $F=J+1$ on both fine-structure levels. However, the available laser power in our experiment is obviously not sufficient to obtain an inversion effect also in the hyperfine component with $F=J-1$. We obtain however $S=0$ on this resonance. On line $2R$ the double-resonance spectrum shows three resonances solely. The upper state $|N=2, K_a=2, J=\frac{5}{2}\rangle$ cannot be excited via an R-branch transition because the corresponding ground state does not exist. We find no inversion effect on this line. It is evident that Hanle measurements are not useful on the lines 2 and $2R$. These lines require definitively an investigation using double-resonance technique.

The results reported before are all obtained using either Hanle measurements or double-resonance measurements with π excitation. These measurements are also performed on several other lines, i.e., on all lines indicated in Table I and some more. However, no inversion effect can be obtained with the available intensity of the laser in our experiment. On several of these lines we find however that the signal S is strongly decreasing with increasing light intensity. In the following we describe double-resonance experiments using σ excitation. Under these conditions the inversion effect is easier obtainable (less light intensity is needed). This will be explained in Sec. IV.

Using double resonance with σ excitation we investigate the inversion effect on lines 3, 4, 7, and 8. Lines 3 and 4 correspond to the excitation of the fine-structure doublet $|N=3, K_a=0, J=3\pm\frac{1}{2}\rangle$, and lines 7 and 8 correspond to the excitation of the fine-structure doublet $|N=4, K_a=1, J=4\pm\frac{1}{2}\rangle$. (The assignment in Refs. 13 and 10 for line 7 is wrong. For corrections compare Ref. 15.) The results on lines 3 and 4 are nearly identical. An inversion effect appears on all three hyperfine components of both lines. The results on lines 7 and 8 are different from those on lines 3 and 4. There is no inversion effect on line 7. There is even no significant decrease of the signal amplitude with increasing light intensity. On the other hand, line 8 shows clearly an inversion effect, but more light intensity is needed than on lines 3 and 4. In connection with these results it is interesting to note the following. As is reported in Ref. 13 the g factors of the states excited on lines 3, 4, 7, and 8 are all in good agreement with the coupling scheme $\hat{J}+\hat{I}=\hat{F}$. On lines 3 and 4 the g factors show also good agreement with the coupling scheme $\hat{N}+\hat{S}=\hat{J}$ (Hund's case b coupling). However, on lines 7 and 8 the g factors indicate no agreement with the coupling scheme $\hat{N}+\hat{S}=\hat{J}$. There is a discrepancy of about 18% between the measured and the calculated (on the basis of the coupling scheme $\hat{N}+\hat{S}=\hat{J}$) g factors on line 8 and a discrepancy of about 53% on line 7. We do not exclude that these results indicate a correlation between the inversion effect and the angular momentum coupling in this molecule.

C. Test experiments

Because the experimental results are novel we check the experimental conditions carefully. From the preceding it is evident that the radiatively decaying states (if there is more than one), which contribute to one observed double-resonance signal for instance, have the same lifetime and g factor. This makes sequential two-photon excitation from the B state of NO_2 to a higher state very unlikely as a possible mechanism of the inversion effect. Excited states of NO_2 which lay at twice the frequency of the visible transition are known, but they do not fluorescence because of predissociation.[3] Nevertheless we perform additional experiments to investigate this possibility. In all experiments the fluorescence light is detected in the spectral range between about 850 nm (limited by the sensitivity of the EMI 9558B photomultipliers) and $\lambda_x=620$ nm. The shorter-wavelength limit is set by filters which transmit only light with wavelengths $\geq\lambda_x$. However, using the transition on line 1 we perform experiments with different filters ($\lambda_x=620$ and 715 nm). These experiments show that the inversion effect is independent of the spectral range of detection. This is an additional argument against a sequential two-photon excitation as a possible cause of the inversion effect.

As a further test we vary the excitation conditions. We change the light intensity either by changing the power of

the pump laser or by inserting neutral density filters in the light path. Both methods give the same results.

The inversion effect depends strongly on the transit time T_L of the molecules through the light field of the laser. To demonstrate this we enlarge the diameter of the laser beam with a beam expander to about 10 mm. The light intensity seems to be approximately constant across the diameter of the beam. However, before the expanded laser beam crosses the molecular beam it passes an adjustable diaphragm. The width of the diaphragm determines now the transit time T_L of the molecules through the light field. Figure 7 shows the measured signal amplitude versus the width of the diaphragm. These results indicate that the inversion effect depends on the product $T_L I$. However, the transit time is inversely proportional to the effective spectral width of the light field seen by the molecules. These results show therefore that the narrower the spectral width of the laser the stronger is the inversion effect.

We perform also an experiment which is approximately the inverse of the previous experiment. We measure the inversion effect simultaneously with two independent lasers which are both tuned to the same transition (line 1). The light beam of the second laser with comparable properties (light intensity, spectral width) to the first laser is directed over a distance of 5 m from an adjacent room to the molecular beam. Both laser beams pass the molecular beam nearly parallel to each other. It is not possible to find any correlation in the inversion effect of the Hanle signal associated with the simultaneous excitation with both lasers. Both lasers seem to contribute independently to the observed signal. If one of the lasers is tuned off-resonance or to another transition we prove that stray light does not influence the inversion effect.

We measure the total fluorescence intensity versus the light intensity at some selected transitions. For instance the transition on line 1 shows proportionality between fluorescence intensity and light intensity up to about 10 mW/mm^2. At a light intensity $I=20$ mW/mm^2 the fluorescence intensity is approximately 20% below the linearly extrapolated value. We conclude from these results that the inversion effect is not directly connected with a laser saturation effect.

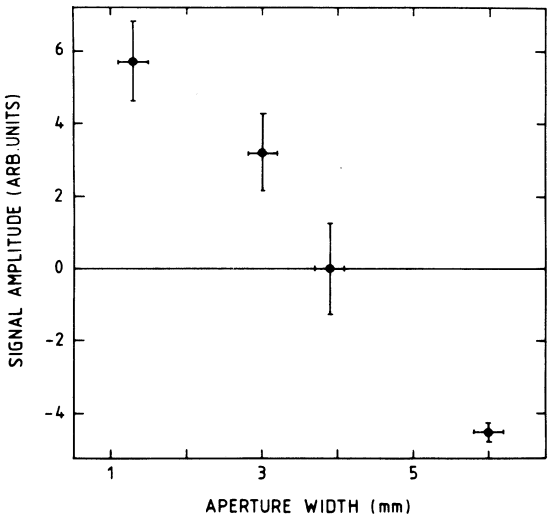

FIG. 7. Signal amplitude vs aperture width. The aperture width determines the transit time of the molecules through the light beam. 1 mm corresponds to about 2×10^{-6} s.

It is very important to know that the molecules are "free." The pressure in the vacuum system is always less than 10^{-5} Torr. We change the NO_2 stagnation pressure in the nozzle between approximately 1 and 400 Torr, and the distance of excitation of the molecules from the nozzle between 0.5 and 2 cm. The inversion effect is independent on these changes. The inversion effect appears also in an experiment under static gas conditions. In this case the environment is totally changed. The molecules are contained in a glass cell. We also try to change the thermal radiation field in which the molecules move. In this case the molecular beam is alternatively shielded with cool (liquid N_2) and hot (700 K) surfaces. However, due to experimental constraints only an effective temperature change of less than 10% is obtainable. This is too low for a detectable effect.

IV. DESCRIPTION OF THE EFFECT

A. The model

It seems necessary to assume an additional process in the molecule between preparation of the excited state and decay by spontaneous emission in order to describe the inversion effect. This follows from all the experience with laser spectroscopy on atoms and molecules where such an effect as reported here was never observed (see, for instance, Refs. 16 and 17). There is an experimental result[18] which at a first glance shows some similarity to our observation. However, the experimental situation is different and enables an explanation different from ours. In order to explain the inversion effect in our experiments we introduce the following phenomenological model, a rationalization of which will be given in the subsequent paper.[6] Laser light induces a transition from a ground state $|a\rangle$ to an excited state $|b\rangle$. However, before $|b\rangle$ decays radiatively, the free molecule evolves in an intramolecular process from $|b\rangle$ to a state $|c\rangle$. Figure 8 shows schematically the states $|a\rangle$, $|b\rangle$, and $|c\rangle$ with the magnetic sublevels $|a,m\rangle$, $|b,m\rangle$, and $|c,m\rangle$. Indicated are also the laser induced transition rate γ_m between the states $|a,m\rangle$ and $|b,m\rangle$, the radiationless decay rate λ_m of $|b,m\rangle$ into $|c,m\rangle$, and the radiative decay rate δ of $|c,m\rangle$. We neglect fluorescence decay of the $|b,m\rangle$ because we assume a rapid radiationless decay of $|b,m\rangle$ into $|c,m\rangle$. Furthermore we neglect any transition of

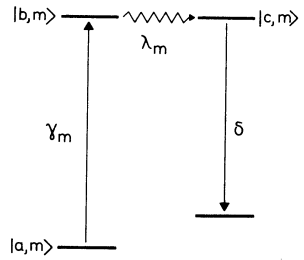

FIG. 8. Schematic representation of the model.

the $|c,m\rangle$ back to the $|b,m\rangle$. This assumption is necessary because fluorescence emission of the state $|b\rangle$ will never contribute to the inversion effect. However, this is a very problematic assumption because it contradicts basic postulates of quantum mechanics. In Ref. 6 we will show how to justify this assumption. We will represent $|c\rangle$ by a many-fold of states having all the same properties, but slightly different energies. $|c\rangle$ represents in this model therefore an intramolecular dissipative quasicontinuum. We have this in mind if we speak of the "state" $|c\rangle$ in the following.

According to the above model the occupation probabilities a_m, b_m, and c_m of the states $|a,m\rangle$, $|b,m\rangle$, and $|c,m\rangle$ follow the rate equations:

$$\dot{a}_m=\beta(a_0-a_m)-\gamma_m(a_m-b_m)\ , \tag{3}$$

$$\dot{b}_m=\gamma_m(a_m-b_m)-\lambda_m b_m\ , \tag{4}$$

$$\dot{c}_m=\lambda_m b_m-\delta c_m\ . \tag{5}$$

Here $\beta(a_0-a_m)$ describes the flow of molecules through the light beam of the laser. In Ref. 6 we will show that λ_m can be written as

$$\lambda_m=\lambda/(1+B\gamma_m)\ , \tag{6}$$

where λ and B are constants. This expression for λ_m follows from the equations of motion of a laser-driven two-level system which interacts irreversibly with a third state $|c\rangle$. This equation means that the decay rate λ_m decreases with increasing intensity of the light field which induced the transition between $|a,m\rangle$ and $|b,m\rangle$. This is the most important step in the explanation of the experimental results. The interaction of the molecule with the light seems to stabilize the state $|b\rangle$ and to lower the radiationless decay rate of $|b\rangle$ into $|c\rangle$. Increasing light intensity thus makes the lifetime of the state $|b\rangle$ effectively longer.

Under stationary state conditions Eqs. (3)—(5) yield

$$c_m=\frac{a_0}{\delta}\frac{\gamma_m}{1+\left[\frac{1}{\lambda}+\frac{1}{\beta}\right]\gamma_m+\left[\frac{B}{\lambda}\right]\gamma_m^2}\ . \tag{7}$$

In the following we discriminate between excitation by P-, Q-, and R-branch transitions. Therefore, we introduce γ_m^α with $\alpha=+1$ for the excitation $F-1\rightarrow F$ (R branch), with $\alpha=0$ for the excitation $F\rightarrow F$ (Q branch) and with $\alpha=-1$ for the excitation $(F+1)\rightarrow F$ (P branch). Here F is the quantum number of the total angular momentum of the excited state. Using the Wigner-Eckart theorem we factorize γ_m^α into

$$\gamma_m^\alpha=x_m^\alpha\gamma^\alpha\ . \tag{8}$$

Here γ^α is independent of the quantum number m. All directional properties are contained in the x_m^α (see, for instance, Ref. 19). For convenience we normalize the x_m^α such that $\sum_x\gamma_m^\alpha=\gamma_\alpha$ with[19]

$$x_m^{+1}=c^{+1}(F^2-m^2),\quad x_m^0=c^0m^2\ ,$$
$$x_m^{-1}=c^{-1}[(F+1)^2-m^2]\ , \tag{9}$$

where the c^α are appropriate normalization constants. An explicit dependence of the γ^α on the quantum numbers N and K_a, for instance, can be derived if we describe the molecular states by symmetric top wave functions.[20] However, we will not do this here because we will show that the results are independent of any assumption on the intrinsic structure of the molecule other than the one introduced in Eqs. (3)—(6). We write Eq. (7) now in the form

$$c_m=\frac{a_0}{\delta}\frac{1}{\frac{1}{\lambda}+\frac{1}{\beta}}\frac{x_m^\alpha DI}{1+x_m^\alpha DI+A(x_m^\alpha DI)^2}\ , \tag{10}$$

where

$$A=\frac{B}{\lambda}\left[\frac{1}{\lambda}+\frac{1}{\beta}\right]^{-2} \tag{11}$$

and

$$DI=\left[\frac{1}{\lambda}+\frac{1}{\beta}\right]\gamma^\alpha\ . \tag{12}$$

Here I designates the measured intensity of the laser light. The constant D depends on the excitation process. It is different for P-, Q-, and R-branch transitions and depends also on the quantum number F. In the following we will show that the amplitude of the signal S [see Eq. (1)] can be expressed as a function of A and DI solely.

B. Observable

We are interested here in the amplitude of the Hanle and double-resonance signals. However, in this section we consider only the double resonance with π excitation. In the Hanle experiment the signal amplitude may be written as $S(0)-S(\infty)$, where $S(0)$ and $S(\infty)$ are the signal S given in Eq. (1) for zero magnetic field and strong magnetic field ($B\approx 50$ mG), respectively. To evaluate $S(0)$ we proceed as follows. The polarization direction of the light beam (direction e_x) is used as quantization axis. a_m, b_m, and c_m are the occupation probabilities of the sublevels $|a,m\rangle$, $|b,m\rangle$, and $|c,m\rangle$ with this choice of the quantization axis. The c_m thus evaluated are given in Eq. (7). To evaluate $S(\infty)$ we use the direction (e_z) of the magnetic field as quantization axis. All off-diagonal matrix elements in this basis vanish because the Zeeman coherence is destroyed in the strong magnetic field. However, $I_x=I_y$ in this case because I_x and I_y are both fluorescence intensities with plane polarization perpendicular to the quantization axis. This gives $S(\infty)=0$. In the double-resonance experiment we write the signal amplitude again as $S(0)-S(\infty)$, but now $S(0)$ means that the magnetic field B is at resonance with the frequency of the rf field, and $S(\infty)$ means that the B field is far off-resonance. In the present case we have $S(0)=0$ because at resonance all c_m are equal and therefore $I_x=I_y$ in Eq. (1). On the other hand, far off resonance we can neglect the rf field and the occupation probabilities of the $|c,m\rangle$ are simply given by Eq. (7). In conclusion the signal amplitude of both the Hanle and the double resonance experiment (with π excitation) are readily evaluated from the

stationary state solution Eq. (7) of the rate equations (3)—(5). Furthermore, we see that the Hanle signal is upward directed if the double-resonance signal is downward directed and vice versa.

Using Eqs. (1) and (2) the desired signal amplitude is

$$S=\frac{\sum_{\epsilon,m} c_m(\delta^{\epsilon}_{x,m}-\delta^{\epsilon}_{y,m})}{\frac{2}{3}\sum_{\epsilon,m} c_m\delta^{\epsilon}} . \tag{13}$$

Here $\delta^{\epsilon}_{x,m}$ and $\delta^{\epsilon}_{y,m}$ are rate constants for fluorescence decay with plane polarization parallel ($\delta^{\epsilon}_{x,m}$) and perpendicular ($\delta^{\epsilon}_{y,m}$) to the electric field vector of the incident light beam, respectively. Therefore, $I_x=\sum_{\epsilon,m} c_m\delta^{\epsilon}_{x,m}$, etc., and $\delta^{\epsilon}=\delta^{\epsilon}_{x,m}+2\delta^{\epsilon}_{y,m}$ is independent on the quantum number m. In Eq. (13) the sum over c_m extends over all orientational sublevels of $|c\rangle$, and the sum over ϵ extends over all P-, Q-, and R-branch transitions in emission with $\epsilon=+1$ for $F\rightarrow F-1$ (R-branch transition in emission), $\epsilon=0$ for $F\rightarrow F$ (Q-branch transition in emission) and $\epsilon=-1$ for $F\rightarrow F+1$ (P-branch transition in emission). Note that a transition that increases F by unity in absorption or decreases F by unity in emission is an R-branch transition, and a transition that decreases F by unity in absorption or increases F by unity in emission is a P-branch transition. As in Eq. (8) we factorize $\delta^{\epsilon}_{x,m}$ and $\delta^{\epsilon}_{y,m}$ into

$$\delta^{\epsilon}_{x,m}=G^{\epsilon}g^{\epsilon}_{x,m},\quad \delta^{\epsilon}_{y,m}=G^{\epsilon}g^{\epsilon}_{y,m} , \tag{14}$$

where G^{ϵ} is independent of m and $g^{\epsilon}_{x,m}$ and $g^{\epsilon}_{y,m}$ are only dependent on F and m. The $g^{\epsilon}_{x,m}$ and $g^{\epsilon}_{y,m}$ are readily evaluated from the equations given in Ref. 19. We obtain

$$\sum_{\epsilon}(\delta^{\epsilon}_{x,m}-\delta^{\epsilon}_{y,m})=\tfrac{1}{2}(G^{+1}-G^{0}+G^{-1})[F(F+1)-3m^2] , \tag{15}$$

$$\sum_{\epsilon}\delta^{\epsilon}=\sum_{\epsilon}(\delta^{\epsilon}_{x,m}+2\delta^{\epsilon}_{y,m})$$
$$=(F+1)[(2F+3)G^{-1}+FG^{0}+2FG^{+1}] .$$

This gives the following expression for S:

$$S=w\frac{\sum_{m} c_m[F(F+1)-3m^2]}{\sum_{m} c_m} \tag{16}$$

with

$$w=\frac{3(G^{+1}-G^{0}+G^{-1})}{(F+1)[(2F+3)G^{-1}+FG^{0}+2FG^{+1}]} . \tag{17}$$

w is independent of the light intensity and is therefore not of direct interest for the present investigation. w can be evaluated if we describe the molecular states by symmetric top wave functions. But we will not do this here. We will solely note that w is important for the strength and the sign (independent of the inversion effect) of the signal in general. All G^{ϵ} are positive. Therefore, $w>0$ if $G^{+1}+G^{-1}>G^{0}$ and vice versa. For molecular states with high quantum numbers K_a, i.e., $K_a\approx N$ we expect $G^{0}>G^{+1}+G^{-1}$ and therefore $w<0$. It may also appear that $G^{+1}+G^{-1}-G^{0}\sim 0$. In this case we see no Hanle or double-resonance signal although a strong absorption line may be present. In the following we use w only as scaling factor for the signal amplitude.

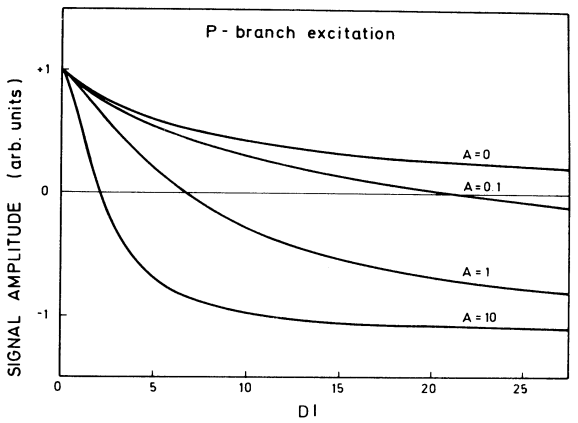

FIG. 9. Signal amplitude vs the quantity DI for different values of A using P-branch excitation for a state with $F=\frac{5}{2}$.

Using the c_m in Eq. (10) we evaluate the signal S, i.e., the amplitude of the Hanle signal and double-resonance signals (with π excitation). Figures 9—12 depict S thus evaluated versus the quantity DI. The "parameter" w is fitted such that $S=1$ for $DI=0$. Figures 9 and 10 depict S for different values of A if a molecular state with $F=\frac{5}{2}$ is excited by a P- or R-branch transition. A calculation was also performed for a Q-branch transition. The results are similar to those of a P-branch transition besides that for a given A we find $S=0$ in the Q-branch transition at about twice the DI value which is needed to obtain $S=0$ in the P-branch transition. This means that the light intensity I must be about a factor of 2 stronger in the Q-branch transition than in the P-branch transition to obtain an inversion effect (if D is the same for both transitions). Note first that an inversion effect cannot appear if $A=0$. For $A=0$ we obtain $S=0$ for $I\rightarrow\infty$ for P-, Q-, and R-branch transitions due to stimulated emission. Second we see that an inversion effect cannot appear even for $A>0$ if the molecular state is excited via the R-branch transition. Only in a P- or Q-branch transition an inversion effect is possible (for a state with $F=\frac{5}{2}$). One can readily see the reason for this. In a state with $F=\frac{5}{2}$ the signal S reads

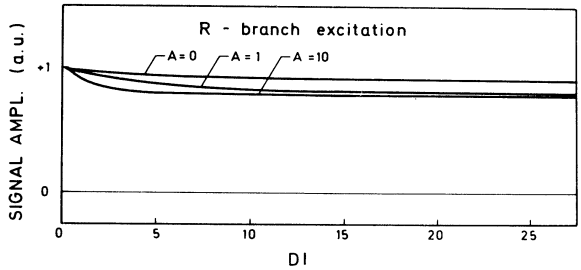

FIG. 10. Signal amplitude vs the quantity DI for different values of A using R-branch excitation for a state with $F=\frac{5}{2}$.

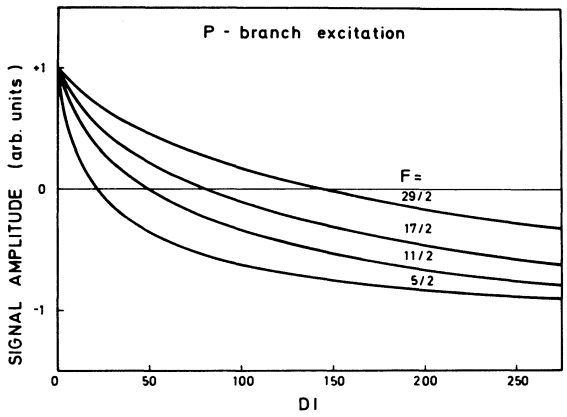

FIG. 11. Signal amplitude vs the quantity DI for different values of the total angular momentum F of the excited state using P-branch excitation. $A=0.1$ in these calculations.

$$S=2w\frac{4c_{1/2}+c_{3/2}-5c_{5/2}}{c_{1/2}+c_{3/2}+c_{5/2}} . \tag{18}$$

Here we use $c_m=c_{-m}$. An inversion effect is only possible if the sublevel with $m=\frac{5}{2}$ is populated. This is however not possible in an R-branch transition.

Figures 9 and 10 show that we cannot expect a high precision in the simultaneous fit of the two parameters A and D to the experimental results. The experimental results can be fitted by A values between $A=0.1$ and 100 if D is appropriately chosen. The value $A=100$ reported before[7,8] is however too big as an estimate of D shows. This estimate is as follows: We assume $\beta<\lambda$ in Eq. (12) with $\beta=1/T_L$, where T_L is the transit time of the molecules through the laser beam. Equation (12) gives therefore $DI=T_L\gamma^{\alpha}$. We estimate γ^{α} using the formula for the transition probability between two states induced by the absorption of radiation from a linearly polarized light beam.[21] Thus we write $\gamma^{\alpha}=|\mu^{\alpha}|^2 IT_L(3\epsilon_0 c_0\hbar^2)$ where we assume that the spectral width of the laser light as seen by the molecules is soley determined by the transit time T_L. The electric dipole transition moment $|\mu^{\alpha}|$ is expressed by $\tau_R^{-1}=\omega_0^3|\mu^{\alpha}|^2(3\pi\hbar\epsilon_0 c_0^3)^{-1}$ where $\tau_R=30$ μs is assumed. This is approximately the radiative decay time in the 593-nm band.[3,4] In the two above formulas c_0 is the velocity of light and ϵ_0 the permittivity of free space.

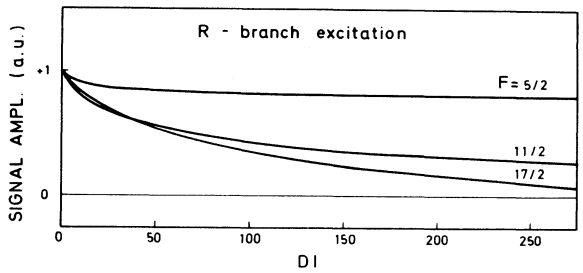

FIG. 12. Signal amplitude vs the quantity DI for different values of the total angular momentum F of the excited state using R-branch excitation. $A=0.1$ in these calculations.

With $T_L=1$ μs we obtain $DI=3I$ (mW/mm^2)$^{-1}$. With this value for D we determine $A=0.1$ from a fit of S to the results (line 1) in Fig. 6. This value for A is also used in the fit of the line $1R$ in Fig. 6.

Figures 11 and 12 depict S versus the quantity DI for excited states with the total angular momentum quantum numbers $F=\frac{5}{2}$, $\frac{11}{2}$, $\frac{17}{2}$, and $\frac{29}{2}$, using P- and R-branch excitation. Here we use again $A=0.1$. The calculation for a Q-branch transition gives similar results as for the P-branch transition. Again the quantity DI must be about a factor of 2 larger in the Q-branch transition than in the P-branch transition to obtain an inversion effect for all F values studied here. We see that is very unlikely even for high quantum number F to find an inversion effect in R-branch excitation.

C. σ Excitation

In the Secs. IV A and IV B the signal amplitude S is evaluated for the Hanle experiment and the double-resonance experiment using π excitation. In the double-resonance experiment using σ excitation the evaluation of the signal amplitude is more difficult, especially the evaluation of λ_m in this case. In the following we consider this experimental condition. The signal is as before given by Eq. (16); however, the c_m have to be evaluated appropriately. As before we have $S=0$ at resonance. To obtain the signal amplitude we need therefore to evaluate the c_m far off-resonance only. This allows us again to neglect the rf field. We assume next that σ excitation is effectively an incoherent excitation of right and left circularly polarized light, if the magnetic field causes a Zeeman splitting in the sublevels $|b,m\rangle$ and $|c,m\rangle$ which exceeds the natural linewidth of these states. With these assumptions we obtain an expression for λ_m and rate equations for the a_m, b_m, and c_m. However, these rate equations are more complicated than Eqs. (3)—(5) because these rate equations couple sublevels with different m. We did not succeed in a useful solution of these rate equations.

The reason why the inversion effect is easier obtainable with σ excitation than with π excitation is obviously the following. The occupation probabilities of the $|b,m\rangle$ represent a stronger angular momentum alignment in the case of π excitation than in the case of σ excitation. It needs therefore less light intensity to invert this alignment using σ excitation as compared to π excitation. A similar situation appeared before when we compared the inversion effect using P-, Q-, or R-branch excitation. For states $|b\rangle$ with low quantum number F we obtain the lowest angular momentum alignment using P-branch excitation. Therefore, the inversion effect is easier obtained for P-branch excitation than for Q-branch excitation for example.

V. CONCLUSION

In this paper we describe a new effect. The degree of polarization of the fluorescence light changes the sign with increasing light intensity. This effect is a direct

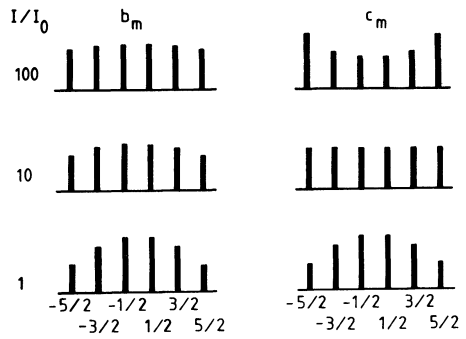

FIG. 13. Schematic representation of the occupation probability distribution of the states $|b,m\rangle$ and $|c,m\rangle$ with $m=\pm\frac{1}{2}$, $\pm\frac{3}{2}$, and $\pm\frac{5}{2}$ for different light intensities I.

consequence of Eq. (6). Owing to the dependence of λ_m on the quantum number m the occupation probability distribution over the sublevels $|b,m\rangle$ and $|c,m\rangle$ which is equal for low light intensity is (under proper conditions of excitations as described before) inverted for high light intensities. This is demonstrated in Fig. 13. This figure shows schematically the occupation probabilities b_m and c_m of the states $|b,m\rangle$ and $|c,m\rangle$ (normalized such that $\sum_m c_m = \sum_m b_m = \text{const}$) for different intensities I of the laser light. For $I=I_0$ the $|b,m\rangle$ and $|c,m\rangle$ have the same occupation probability distribution. For $I=10I_0$ all c_m are equal, that is $S=0$ at this light intensity. Finally for $I=100I_0$ the c_m represent an occupation probability distribution which is inverse to the occupation probability distribution for $I=I_0$. This will never appear for the b_m. At the extreme case all b_m can be equal for high light intensities I.

Equation (6) describes what we suggest be named "light-induced stability" of an excited molecular state. The state $|b\rangle$ gains stability from the interaction with the laser light. We have seen that the effect of the laser light is not only a question of intensity. The spectral width and therefore the coherence in the light field seem to be as important as the light intensity. As is well known from solutions of the optical Bloch equations for a two level system (see, for instance, Refs. 1,2) strong light intensity of a narrow band laser induces a state which is a coherent superposition of the $|a,m\rangle$ and $|b,m\rangle$. In a subsequent paper[6] we derive Eq. (6). We will show how it is connected with the coherence between the $|a,m\rangle$, $|b,m\rangle$, and $|c,m\rangle$. In Ref. 6 we will discuss also the question of irreversibility. We will show that Eq. (6) follows directly from the assumption of an irreversible transition from $|b\rangle$ to $|c\rangle$. Therefore, the effect described in this paper seems to be intimately connected with the time evolution of the isolated molecule in an electronically excited state.

ACKNOWLEDGMENT

This work was supported by the Deutsche Forschungsgemeinschaft.

[1]C. Cohen-Tannoudji, in *Frontiers in Laser Spectroscopy,* edited by R. Balian, S. Haroche, and S. Liberman (North-Holland, Amsterdam, 1977), Vol. 1.

[2]L. Allen and J. Eberly, *Optical Resonances and Two-Level Atoms* (Wiley, New York, 1975).

[3]D. K. Hsu, D. L. Monts, and R. N. Zare, *Spectral Atlas of Nitrogen Dioxide* (Academic, New York, 1978).

[4]E. K. C. Lee and G. L. Loper, in *Radiationless Transitions,* edited by S. H. Lin (Academic, New York, 1980).

[5]W. Happer and R. Gupta, in *Progress in Atomic Spectroscopy, Part A,* edited by W. Hanle and H. Kleinpoppen (Plenum, New York, 1978).

[6]H. G. Weber (unpublished).

[7]F. Bylicki and H. G. Weber, Phys. Lett. **100A**, 182 (1984).

[8]F. Bylicki, H. G. Weber, and H. Zscheeg, Z. Phys. A **314**, 123 (1983).

[9]M. Arnold, F. Bylicki, H. G. Weber, and H. Zscheeg, in *Proceedings of the Eighth Colloquium on High Resolution Molecular Spectroscopy, Tours, France, September, 1983,* edited by Ch. Bordé (Université Paris-Nord, Paris, 1983).

[10]F. Bylicki and H. G. Weber, J. Chem. Phys. **78**, 2844 (1983).

[11]C. G. Stevens and R. N. Zare, J. Mol. Spectrosc. **56**, 167 (1975).

[12]T. Tanaka, R. W. Field, and D. O. Harris, J. Mol. Spectrosc. **56**, 188 (1975).

[13]F. Bylicki, G. Miksch, and H. G. Weber (unpublished).

[14]S. Gerstenkorn and P. Luc, Atlas du Spectre d'Absorption de la Molécule d'Iode 14 800–20 000 cm^{-1}, édition du Centre National de la Recherche Scientifique, Paris 1978.

[15]F. Bylicki, H. G. Weber, H. Zscheeg, and M. Arnold, J. Chem. Phys. 80, 1791 (1984).

[16]B. Decomps, M. Dumont, and M. Ducloy, in *Laser Spectroscopy of Atoms and Molecules,* Vol. 2 of *Topics in Applied Physics,* edited by H. Walther (Springer, Berlin, 1970).

[17]H. Walther, in *Laser Spectroscopy of Atoms and Molecules,* Vol. 2 of *Topics in Applied Physics,* edited by H. Walther (Springer, Berlin, 1970).

[18]M. P. Gorza, B. Decomps, and M. Ducloy, Opt. Commun. **8**, 323 (1973).

[19]E. U. Condon and G. H. Shortely, *The Theory of Atomic Spectra* (Cambridge University Press, Cambridge, 1970).

[20]D. C. Cross, R. M. Hainer, and G. W. King, J. Chem. Phys. **12**, 210 (1944).

[21]O. Svelto, *Principles of Lasers* (Plenum, New York, 1976), Chap. 2.